

4E Binding Proteins Inhibit the Translation Factor eIF4E without Folded Structure<sup>†</sup>C. Mark Fletcher,<sup>‡</sup> Abigail M. McGuire,<sup>‡</sup> Anne-Claude Gingras,<sup>§</sup> Hanjun Li,<sup>‡</sup> Hiroshi Matsuo,<sup>‡</sup> Nahum Sonenberg,<sup>§</sup> and Gerhard Wagner<sup>\*,‡</sup>*Department of Biological Chemistry and Molecular Pharmacology, Harvard Medical School, Boston, Massachusetts 02115, and Department of Biochemistry and McGill Cancer Center, McGill University, Montréal, Québec H3G 1Y6, Canada**Received October 8, 1997; Revised Manuscript Received November 12, 1997<sup>®</sup>*

**ABSTRACT:** The 4E binding proteins (4E-BP1 and 4E-BP2) inhibit translation by binding to the limiting, proto-oncogenic initiation factor eIF4E. 4E-BPs produced in *Escherichia coli* had little or no folded structure, measured by NMR and CD. However, these proteins inhibited translation in reticulocyte lysate. Furthermore, they bound to isolated mouse eIF4E, showing a few broader, dispersed new NMR signals but no general increase in chemical shift dispersion. A peptide with the sequence of 4E-BP1 residues 49–68 was sufficient to bind eIF4E and to inhibit translation in reticulocyte lysate. These results suggest that a short central region of the 4E-BPs is responsible for eIF4E binding and translation inhibition while the remainder is unfolded and flexible.

The 4E binding proteins (4E-BP1 and 4E-BP2) regulate translation by inhibiting formation of the initiation factor complex eIF4F (1). This complex consists of three components: eIF4E, the 25 kDa cap binding protein; eIF4A, a 45 kDa RNA helicase; and eIF4G, a larger protein that binds together eIF4E, eIF4A and other components of the translation machinery. eIF4F is thought to unwind secondary structure in the 5' untranslated region of the mRNA and mediate binding of the 40S ribosomal subunit (2). eIF4E, the limiting component of the complex, is an important point of translational regulation (3). This regulation is central to the control of cell growth, since for the cell to proceed through the cell cycle requires a general increase in translation in response to growth factors, hormones and other mitogens (4).

The activity of the 4E-BPs is modulated by phosphorylation. In the underphosphorylated form, 4E-BPs compete with eIF4G for binding to eIF4E at the same site, thereby inhibiting formation of eIF4F (1, 5, 6). The eIF4E binding regions of the 4E-BPs and eIF4G have similar amino acid sequences (Figure 1). Upon hyperphosphorylation, 4E-BPs are no longer capable of binding eIF4E, leading to an increase in translation (1). 4E-BP1 has 5–10 serine and threonine phosphorylation sites and 4E-BP2 has at least two such sites (7–9; Gingras and Sonenberg, unpublished data). It is not known which sites are responsible for dissociation from eIF4E.

4E-BPs are phosphorylated in response to growth factors and mitogens (1, 10). Furthermore, the rapamycin sensitive

4E-BP1	MSGGSSCSQTP--SRAIPATRRVVLGDGVLPFGDYSTTPGGT	1-41
4E-BP2	MSSSAGSGHQPSQSRAIP-TRTVAISDAALPH-DYCTTPGGT	1-41
4E-BP1 (human)	LFSTTPGGTRIIYDRKFLMECRNSFVTKTPPDLPTIPGVTSF	42-84
4E-BP2 (human)	LFSTTPGGTRIIYDRKFLMDRRNSFMAQTFFCHLPNIPGVTSF	42-84
Human eIF4G	KKRYDREFLLGQFIF	413-428
Yeast eIF4G	KYTYGPTPLQLQFKDL	449-464
p20 (yeast)	MIKYTIDELFQLKPSL	1-16
4E-BP1	SS--DEPPMEASQSHLRNSPEDKRAAGGEESEFMDI	95-118
4E-BP2	GTLIEDSKVEVNNLNHNHDKHAGVGDQAQFMDI	95-120

FIGURE 1: Sequences of 4E-BPs and homologous regions of p20 and eIF4G. Human and *S. cerevisiae* eIF4G contain a short stretch of homology to the 4E-BPs, as shown here. Both the whole conserved region and the individual tyrosine and leucine residues are essential for eIF4E binding by the 4E-BPs and eIF4Gs (6). p20, the *S. cerevisiae* equivalent of the 4E-BPs, contains a similar motif at its N-terminus (41).

pathway involving the mTOR/FRAP kinase seems to be involved in the phosphorylation event that leads to dissociation from eIF4E (11–15). This pathway is stimulated by growth factors, hormones and other mitogens, all of which cause a general increase in translation (16). Recent work suggests that 4E-BPs may be phosphorylated directly by mTOR (17). eIF4E, eIF4G, and other translation factors are also regulated by phosphorylation (2, 3) but the importance of the 4E-BPs is indicated by the shutdown of host cell translation that occurs upon encephalomyocarditis virus infection, which is caused by 4E-BP dephosphorylation (18).

Overexpression of eIF4E transforms cells in culture, consistent with its central role in the control of cell growth (reviewed in ref 3). A possible mechanism is translational upregulation of growth factor mRNAs, many of which have highly structured 5' untranslated regions that should respond strongly to eIF4F's RNA helicase activity. Increased levels of such growth factors are indeed seen in cells transformed by eIF4E (reviewed in ref 3).

<sup>†</sup> This work was supported by NIH Grant CA68262 to G.W. C.M.F. was supported by fellowships from NATO and the International Human Frontier Science Program, A.M.M. by a Howard Hughes Medical Institute predoctoral fellowship and A.-C.G. by a National Science and Engineering Research Council 67 studentship.

<sup>\*</sup> Author to whom correspondence should be addressed.

<sup>‡</sup> Harvard Medical School.

<sup>§</sup> McGill University.

<sup>®</sup> Abstract published in *Advance ACS Abstracts*, December 15, 1997.

Although eIF4E is not proven to be a primary oncogene *in vivo*, elevated levels of this protein are observed in breast cancers and cultured tumor cells (19, 20). This suggests that drugs or other therapies to reduce eIF4E activity to normal levels might be effective in controlling tumor growth. The importance of the 4E-BPs is shown by the fact that their overexpression partially reverses the transformed phenotype caused by eIF4E (21). The 4E-BPs therefore provide a natural model for inhibitors of eIF4E.

4E-BP1 and 4E-BP2 are proteins of 118 and 120 residues, respectively, with 56% sequence identity (Figure 1; 1). No functional differences between the two proteins have been identified, but their tissue distribution varies (22). Mouse and rat homologues of both proteins have been identified and have greater than 90% amino acid identity in each case (10, 11, 22–24).

Here, we investigate the structure of the 4E-BPs. We prepared recombinant 4E-BP1 and 4E-BP2 protein constructs. NMR and CD measurements indicated that these proteins were not folded in approximately physiological solution conditions. However, the same protein samples were able to inhibit translation in reticulocyte lysate, as observed for previous recombinant 4E-BP constructs (1). Upon titrating the proteins with eIF4E and recording NMR spectra, we discovered that most or all of the unfolded 4E-BP bound to eIF4E, showing a few broader, dispersed peaks but no general increase in chemical shift dispersion. To confirm this result we obtained a 20 residue peptide fragment of 4E-BP1 containing the eIF4E binding motif. This peptide bound to eIF4E, producing similar chemical shift changes to the full-length 4E-BP1, and inhibited translation in reticulocyte lysate. Together, these results suggest that a short central region of the 4E-BPs is responsible for eIF4E binding and translation inhibition while the flanking regions are unfolded and flexible.

## EXPERIMENTAL PROCEDURES

**Preparation of 4E-BP1.** *Escherichia coli* strain BL21- (DE3) was transformed with pGEX-2T-4EBP1 plasmid (1) and grown on M9 minimal medium (containing 0.5 g/L  $^{15}\text{NH}_4\text{Cl}$  or  $\text{NH}_4\text{Cl}$  and 4 g/L glucose as the sole nitrogen and carbon sources) at 37 °C to an  $\text{OD}_{600}$  of 1.0. Expression was induced by the addition of IPTG to 0.5 mM and the cells grown for a further 6 h before harvesting. Cells were resuspended in 20 mM  $\text{NaH}_2\text{PO}_4/\text{Na}_2\text{HPO}_4$ , pH 7.3, 150 mM NaCl, 10 mM EDTA, 0.2 mM PMSF, and 0.1% Triton X-100, treated with 0.5 mg/mL lysozyme, 10 mM  $\text{MgCl}_2$ , and 5  $\mu\text{g}/\text{mL}$  DNase I, and sonicated. After centrifugation, the supernatant was mixed with glutathione sepharose 4B (Pharmacia) in a batch procedure. The resin was washed three times with resuspension buffer and three times with 50 mM Tris/HCl, pH 7.5, 150 mM NaCl, and 2.5 mM  $\text{CaCl}_2$ . The 4E-BP1 moiety was cleaved from the bound GST by incubation with 0.5 unit/mL thrombin (Boehringer Mannheim) for 2 h at 20 °C, followed by quenching with excess PMSF and EDTA. The protein was eluted, concentrated and purified further by FPLC on a Pharmacia Superdex-75 gel filtration column in NMR buffer. The final protein was greater than 95% pure as estimated from Coomassie blue stained SDS-PAGE with the only visible impurity being thrombin which was irreversibly inhibited and not  $^{15}\text{N}$ -

labeled. The identity of the protein was confirmed by N-terminal sequencing and mass spectrometry.

**Preparation of 4E-BP2.** *E. coli* strain SG13009[pREP4] (Qiagen) was transformed with the plasmid pQE31-4EBP2His (25), grown at 37 °C, and expression induced by the addition of IPTG to 2 mM. On rich media, expression was induced at an  $\text{OD}_{600}$  of 0.7 and the cells grown for a further 2 h at 37 °C; on minimal medium expression was induced at an  $\text{OD}_{600}$  of 0.4 and the cells grown for a further 1 h at 25 °C in the presence of 0.2 mM PMSF. Pelleted cells were generally resuspended in buffer A (8 M urea, 100 mM  $\text{NaH}_2\text{PO}_4/\text{Na}_2\text{HPO}_4$ , pH 8.0, 10 mM Tris/HCl, 10 mM  $\beta$ -mercaptoethanol, 0.5 mM PMSF, and 0.5  $\mu\text{g}/\text{mL}$  leupeptin and pepstatin) and lysed by stirring for 1 h. After centrifugation, the supernatant was mixed with Ni-NTA resin (Qiagen) which was washed with buffer B (as A except pH 6.3 and including 0.5 M NaCl). 4E-BP2 was eluted with buffer C (as A except pH 4.5). In one case, cells were resuspended in buffer D (50 mM  $\text{NaH}_2\text{PO}_4/\text{Na}_2\text{HPO}_4$ , pH 8.0, 300 mM NaCl, 10 mM  $\beta$ -mercaptoethanol, 0.5 mM PMSF, 0.5  $\mu\text{g}/\text{mL}$  leupeptin and pepstatin, and 0.1% Triton X-100) and lysed by sonication. After centrifugation, the supernatant was mixed with Ni-NTA resin which was washed with buffer E (as D except pH 6.0). 4E-BP2 was eluted with a gradient of 0 to 0.5 M imidazole in buffer E. In all cases, the protein was then dialyzed into 20 mM  $\text{NaH}_2\text{PO}_4/\text{Na}_2\text{HPO}_4$ , pH 6.0, 10 mM DTT, and 0.5 mM PMSF. An impurity of approximately 28 kDa was removed using a POROS HQ/H column (PerSeptive Biosystems) to which it bound but 4E-BP2 did not. Finally, two degradation products of approximately 8–10 kDa were removed using a Sephadex G-50 gel filtration column (Pharmacia) in NMR buffer. The final protein was greater than 98% pure as estimated from silver stained SDS-PAGE. The identity of the protein was confirmed by N-terminal sequencing. Although the protein gave three closely spaced bands on SDS-PAGE, mass spectrometry indicated a single major species of the expected molecular weight.

**Translation Inhibition Assays.** Reticulocyte lysate assays were carried out as previously described (1). In the experiment shown in Figure 5, nuclease treated reticulocyte lysate (Promega; 8  $\mu\text{L}$  per reaction) was incubated in a total volume of 15  $\mu\text{L}$  according to the manufacturer's instructions. Histidine tagged rat 4E-BP1 or peptide was resuspended in translation buffer (10 mM HEPES, pH 7.5, 75 mM KAc, 25 mM KCl, 2 mM  $\text{MgCl}_2$ , 2 mM DTT, and 0.1 mM EDTA) and added to the reactions in the indicated amounts. Each reaction included 75 ng of capped CAT mRNA produced by *in vitro* transcription, kindly provided by H. Imataka. [ $^{35}\text{S}$ ]Methionine was added to the mixtures and translation performed for 60 min at 30 °C. The reaction was stopped by the addition of Laemmli sample buffer and the products separated by SDS-PAGE. The gel was processed for fluorography using En $^3$ Hance (Dupont) and quantified with a phosphorimager (Fuji).

**Preparation of Complexes.** Mouse eIF4E was produced in *E. coli* and purified using  $\text{m}^7\text{GDP}$ -agarose as previously described (26, 27). Complexes of eIF4E and 4E-BP or peptide were produced by preparing the individual proteins in identical buffers and mixing them directly. The buffer was typically 20 mM HEPES, pH 6.5, 0.3 M L-arginine hydrochloride, 100 mM KCl, 2.5 mM  $\text{MgCl}_2$ , 1 mM DTT,

0.5 mM EDTA, and 0.2–5.0 mM  $m^7$ GDP. The unlabeled species was added in 2–5 steps, concentrating the sample before recording the next spectrum if necessary, until no further changes were observed in the  $^{15}\text{N}$  HSQC spectrum. All NMR spectra in a given titration experiment were acquired and processed in an identical manner.

In one case, an eIF4E:4E-BP1 complex was purified as follows. Approximately 15–20 mg of unlabeled eIF4E was purified on  $m^7$ GDP-agarose using the normal procedure up to and including the GDP washing step. The column was then washed with 20 mM HEPES, pH 7.5, 100 mM KCl, 2.5 mM  $\text{MgCl}_2$ , 1 mM DTT, and 0.5 mM EDTA before applying approximately 9 mg of purified  $^{15}\text{N}$ -labeled 4E-BP1 in the same buffer. Unbound material was washed away before eluting with 200  $\mu\text{M}$   $m^7$ GDP in the same buffer. The resulting mixture was concentrated and purified by FPLC on a Pharmacia Superdex-75 gel filtration column. A minimal number of fractions containing the complex were pooled and concentrated for NMR measurements.

**NMR Measurements.** NMR sample concentrations were 0.2–0.6 mM (of the  $^{15}\text{N}$ -labeled component in the case of complexes). A typical buffer was 50 mM  $\text{NaH}_2\text{PO}_4/\text{Na}_2\text{HPO}_4$ , pH 6.5, 100 mM NaCl, 1 mM DTT, and 1 mM  $\text{NaN}_3$  in 90%  $\text{H}_2\text{O}/10\%$   $\text{D}_2\text{O}$ . Spectra were recorded on Bruker AMX 500 and 600 MHz and Varian UnityPlus 750 MHz spectrometers. Unless otherwise stated, the temperature was 25 or 27  $^\circ\text{C}$ .  $^{15}\text{N}$  HSQC spectra were recorded with WATERGATE-HSQC or FHSQC pulse sequences (28, 29), 64–256  $t_1$  increments and 64–512 scans per increment.  $^{15}\text{N}$  2D NOESY-HSQC spectra (30) were recorded with 150 ms mixing time, 192  $t_1$  increments and 128 scans. A 2D NOESY spectrum (31) was recorded with 150 ms mixing time, 512  $t_1$  increments and 64 scans. NMR data were processed and displayed using Felix (Biosym Technologies).

**CD Measurements.** CD spectra were recorded on an Aviv 62DS spectropolarimeter at 25  $^\circ\text{C}$  unless otherwise stated. Samples contained approximately 20  $\mu\text{M}$  4E-BP1 in 20 mM HEPES, pH 6.5, 0 or 8 M urea, 100 mM KCl, 2.5 mM  $\text{MgCl}_2$ , 1 mM DTT, and 0.5 mM EDTA.

## RESULTS

### 4E-BPs Have Little or No Folded Structure in Solution.

4E-BP1 and 4E-BP2 proteins were expressed in *E. coli* and purified, either uniformly labeled with  $^{15}\text{N}$  or unlabeled. The 4E-BP1 construct lacked the three N-terminal residues of the native sequence and had a substitution of proline for serine at the third position. The 4E-BP2 construct contained an N-terminal histidine tag of the sequence MRGSHHHH-HHTDPA.

1D and 2D NMR spectra of these proteins displayed very limited  $^1\text{H}$  chemical shift dispersion: no NH signals above 8.7 ppm, no  $\text{C}^{\alpha}\text{H}$  signals above 5.0 ppm, and no methyl signals below 0.5 ppm (Figure 2A). Furthermore, the 2D NOESY spectrum of 4E-BP2 and  $^{15}\text{N}$  2D NOESY-HSQC spectra of both proteins contained few cross-peaks, none of which could be identified as inter-residue connectivities indicative of secondary structure (e.g., strong  $d_{\text{NN}}$  cross-peaks) or tertiary structure (e.g., cross-peaks between aromatic ring and aliphatic side chain protons). We concluded that the purified 4E-BPs have little or no folded structure in solution.

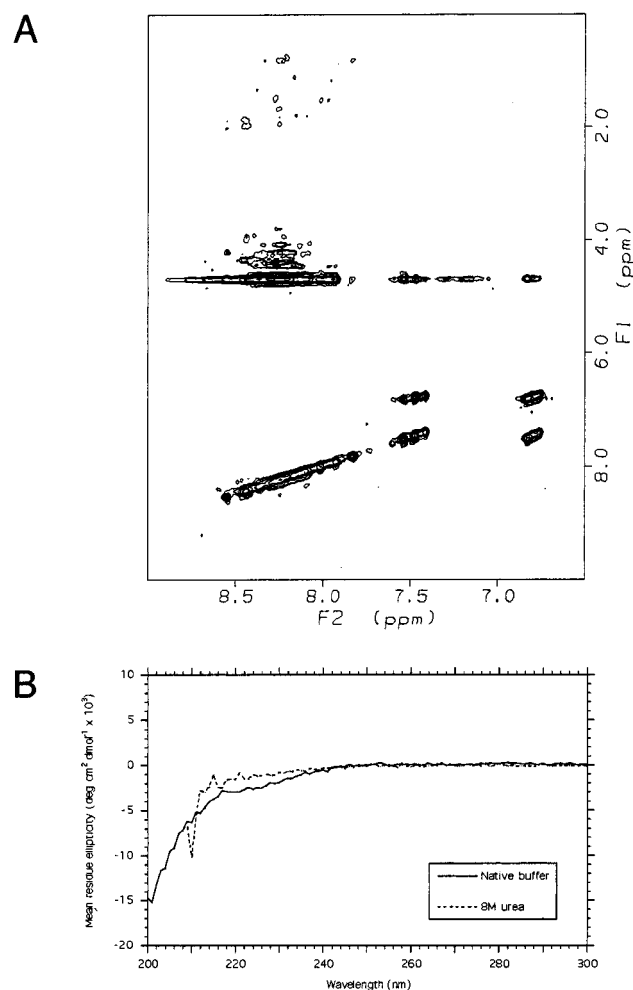


FIGURE 2: 4E-BPs have little or no folded structure in solution. (A) 600 MHz  $^{15}\text{N}$  2D NOESY-HSQC spectrum of 4E-BP1. No more cross-peaks were observed at lower contour levels. This spectrum was recorded with a NOESY mixing time of 150 ms, 128 scans per  $t_1$  increment and a total measuring time of approximately 2 days. (B) CD spectra of 4E-BP1 recorded in the presence and absence of 8 M urea. In both cases a spectrum of the buffer alone (without protein) was subtracted. In 8 M urea no data was recorded below 208 nm due to interference from the buffer.

This is true under various conditions of temperature and pH, since the  $^1\text{H}$  1D spectrum of 4E-BP2 did not change significantly over the temperature range 7–42  $^\circ\text{C}$  (5  $^\circ\text{C}$  steps; pH 6.5) and at pH 6.5, 7.0, 7.5, and 8.5 (27  $^\circ\text{C}$ ). Although 4E-BP2 was generally purified in 8 M urea and dialyzed into nondenaturing solution conditions, the protein purified entirely under nondenaturing conditions gave an identical  $^1\text{H}$  1D spectrum. The NMR spectra of the 4E-BPs displayed sharp lines, which is also consistent with the proteins being unfolded and therefore very mobile.

It is possible for a protein to have helical secondary structure but to show little  $^1\text{H}$  chemical shift dispersion, which would also make it difficult to observe the expected  $d_{\text{NN}}$  sequential NOE connectivities (32). We therefore made CD measurements, which are very sensitive to helical structure (33). The CD spectrum of 4E-BP1 is typical of an unfolded protein, although a very shallow minimum at 220–230 nm suggests a minimal amount of helical secondary structure (Figure 2B). Furthermore, the spectrum changes little upon addition of urea to 8 M (although the shallow minimum disappears) and the ellipticity at 220 nm is constant

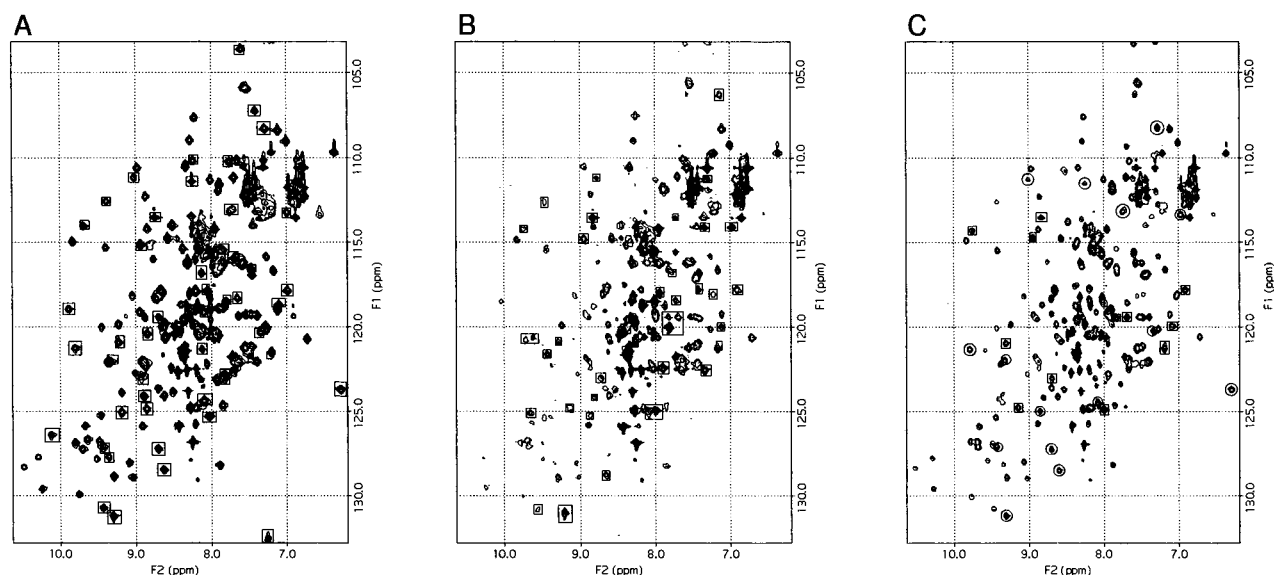


FIGURE 3: eIF4E binds unfolded 4E-BPs and a 20 residue fragment of 4E-BP1. 750 MHz  $^{15}\text{N}$  HSQC spectra of eIF4E: (A) alone, (B) fully titrated with unlabeled 4E-BP1, (C) fully titrated with the 20 residue 4E-BP1 fragment. Boxed peaks in panel A move or disappear upon addition of 4E-BP1, boxed peaks in panel B appear upon addition of 4E-BP1. In panel C, peaks in boxes appear upon addition of the peptide, as upon addition of 4E-BP1; peaks in circles moved or disappeared upon addition of 4E-BP1 but did not change upon addition of the peptide, i.e., they are the same as in the free eIF4E. A number of slighter changes are not indicated here. These spectra were acquired and processed identically, except that the contour levels in panel B are one-third of those in panels A and C. We recorded 112 scans per  $t_1$  increment and the measuring time for each spectrum was approximately 21 h.

over the temperature range 20–90 °C (5 °C steps), indicating that the protein is unfolded under nondenaturing solution conditions.

**Unfolded 4E-BPs Inhibit Translation In Vitro.** The discovery that histidine tagged 4E-BP2 was unfolded was surprising, since this protein, and also the intact GST-4E-BP1 fusion protein, had previously been shown to inhibit translation in reticulocyte lysate and to bind mouse eIF4E in far western experiments (1; Gingras and Sonenberg, unpublished data). However, we confirmed that the unfolded protein constructs were active. In reticulocyte lysate assays, our samples of 4E-BP1 and 4E-BP2 inhibited translation in a dose-dependent manner and this was overcome by addition of purified eIF4E (all the experiments described in this paper used mouse eIF4E, which is 99.5% identical to the human protein). This data is not shown since it is identical to previously published results except for the precise sequences of the protein constructs.

It is conceivable that this inhibition was caused by a small fraction of the protein that was correctly folded but was not detected in the NMR or CD spectra. It is also conceivable that the 4E-BPs become folded under the conditions of the assay, perhaps due to interaction with eIF4E. Both of these possibilities were addressed by the following experiments.

**Unfolded 4E-BPs Bind to eIF4E.** We prepared recombinant 4E-BPs and eIF4E in identical buffers, with one component  $^{15}\text{N}$ -labeled and the other unlabeled, and recorded  $^{15}\text{N}$  HSQC spectra upon addition of increasing amounts of the unlabeled component to the NMR sample. Titration was continued until no further changes were observed.

The eIF4E spectrum showed many changes upon addition of an approximately equimolar amount of 4E-BP1. Figure 3A shows the  $^{15}\text{N}$  HSQC spectrum of free eIF4E: peaks that disappeared upon addition of 4E-BP1 are boxed. Figure 3B shows the spectrum of eIF4E after complete titration with 4E-BP1: new peaks are boxed. Furthermore, small but clear

changes were observed in the spectra of both 4E-BPs upon addition of an approximately equimolar amount of eIF4E (Figure 4). We concluded that most or all of the unfolded 4E-BP in our samples binds to eIF4E. The broader lines observed for eIF4E upon addition of 4E-BP1 are consistent with the formation of a complex.

In the titration of  $^{15}\text{N}$ -labeled 4E-BP1, eIF4E was added in many small increments. This data shows that the changes involve only the disappearance of peaks and the appearance of new ones and not the stepwise movement of peaks to new positions, i.e., that the complex is in slow exchange. This indicates that the off-rate is small ( $k_{\text{OFF}} < 0.1 \text{ s}^{-1}$ ) and is typical of fairly tight binding ( $K_D < 10 \mu\text{M}$ ).

**Binding to eIF4E Does Not Cause Folding.** Although there are changes in the  $^{15}\text{N}$  HSQC spectra of both 4E-BPs upon addition of eIF4E, there is no dramatic increase in the chemical shift dispersion (Figure 4). Furthermore, the  $^{15}\text{N}$  2D NOESY-HSQC spectrum of 4E-BP1 fully titrated with eIF4E shows no more NOE cross-peaks than the spectrum of the free protein (data not shown). Therefore the 4E-BPs appear to remain mainly or completely unfolded upon binding to eIF4E. The majority of signals in the spectra of complexed 4E-BPs have sharp lines, which is also consistent with the molecules being unfolded and mobile.

Upon complex formation, both 4E-BP  $^{15}\text{N}$  HSQC spectra show a small number of weak new peaks dispersed upfield from the majority of other signals (Figure 4). This does not seem sufficient to indicate extensive folding of the 4E-BPs upon binding, but rather seems likely to result from the interaction of a small number of residues with eIF4E or from a small region of the 4E-BPs becoming structured (or both). The weakness of these signals is consistent with the binding residues being less mobile than the remainder of the protein.

In 4E-BP1, these new signals include a pair of peaks with the same  $^{15}\text{N}$  chemical shift and in the appropriate region for a side chain amide group of asparagine or glutamine,

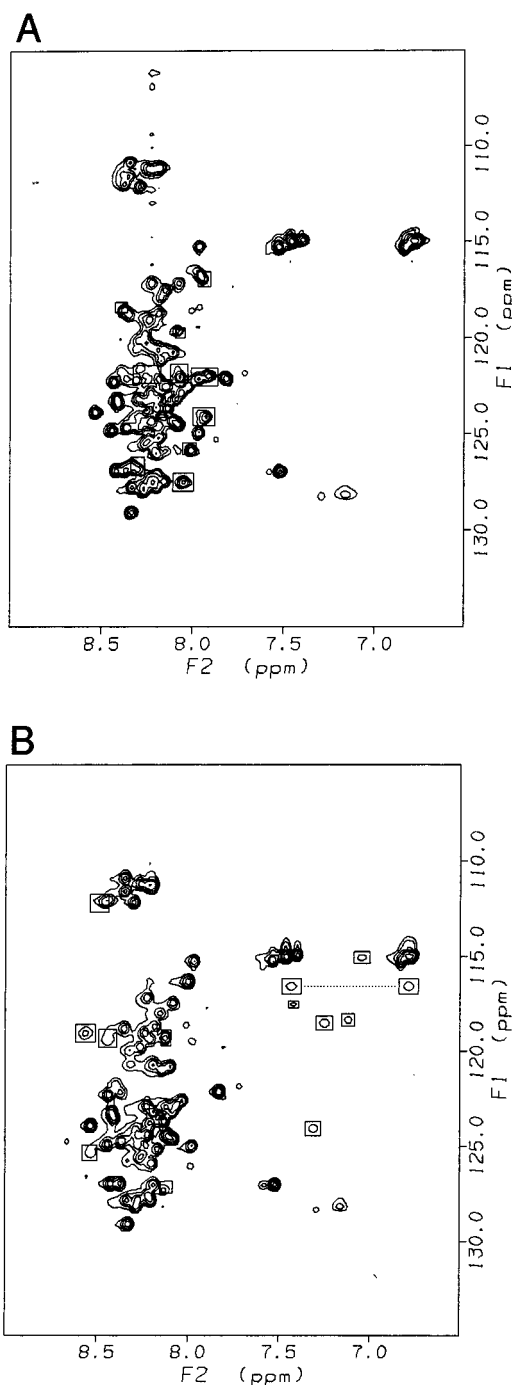


FIGURE 4: Binding to eIF4E does not cause folding. 600 MHz  $^{15}\text{N}$  HSQC spectra of 4E-BP1: (A) alone, (B) fully titrated with unlabeled eIF4E. Boxed peaks in panel A move or disappear upon addition of eIF4E, boxed peaks in panel B appear upon addition of eIF4E. A number of slighter changes are not indicated here. The dotted line connects the two signals from a side chain  $\text{CONH}_2$  group (see Results). These spectra were acquired and processed identically. We recorded 128 scans per  $t_1$  increment and the measuring time for each spectrum was approximately 10 h. Similar results were obtained with 4E-BP2.

indicating that such a group is involved in the interaction with eIF4E. The eIF4E binding region contains no glutamines and a single asparagine (residue 64; see Figure 1).

Although the eIF4E binding region of the 4E-BPs contains conserved arginine residues, none of the weak new cross-peaks in the eIF4E:4E-BP1 complex are from arginine side chains. This was deduced from a  $^{15}\text{N}$  HSQC spectrum of

the complex recorded with a wider  $^{15}\text{N}$  spectral width to identify arginine side chain signals that were folded in previous spectra. Note that this does not rule out the involvement of undetected arginine side chains in the interaction.

It follows that, with the exception of the side chain amide cross-peaks, all of the weak new signals come from backbone amide groups. Assuming that in the free protein these signals are located in the central mass of strong peaks, their new positions imply upfield  $^1\text{H}$  chemical shift changes of approximately 0.5 ppm or more. This could result from changes in position relative to nearby aromatic rings: the eIF4E binding region of the 4E-BPs contains conserved phenylalanine and tyrosine residues (Figure 1) while the 4E-BP binding surface of yeast eIF4E includes aromatic residues that are conserved in mammalian eIF4E (27). An alternative explanation for the upfield shifts is the formation of a small  $\alpha$ -helix (32).

It was desirable to confirm that the intriguing spectra we observed for the complexed 4E-BPs represented 100% bound protein and not some mixture of bound and free, perhaps aggregated, protein. To this end, we purified the eIF4E:4E-BP1 complex as a single species, using  $m^7\text{GDP}$ -agarose affinity and gel filtration chromatography, to obtain as nearly as possible a 1:1 ratio of the two proteins. The  $^{15}\text{N}$  HSQC spectrum of 4E-BP1 in this complex was identical to those obtained from the titration experiments.

Finally, note that although our data show that binding of 4E-BPs to eIF4E does not require a folded structure at any stage, it is possible that the full inhibitory effect of the 4E-BPs requires structure that we have not observed.

*A 20 Residue Fragment of 4E-BP1 Binds to eIF4E and Inhibits Translation in Vitro.* The results described above suggested a model in which a small region of the 4E-BP binds to eIF4E and the remainder is flexible and unfolded. To investigate this possibility further, we obtained a synthetic peptide with the sequence of 4E-BP1 residues 49–68. This includes the conserved motif necessary for eIF4E binding and translation inhibition.

Titration of  $^{15}\text{N}$ -labeled eIF4E with this peptide produced some, but not all, of the same chemical shift changes as the whole 4E-BP1 (Figure 3C). This indicates that the peptide binds to eIF4E, although it suggests that the peptide does not make as many contacts or bind in quite the same way as the whole 4E-BP1. Furthermore, in reticulocyte lysate assays, the peptide inhibited translation in a dose-dependent manner (Figure 5). These experiments used full-length 4E-BP1 as a positive control and were reproducible.

Thus, residues 49–68 of 4E-BP1 are sufficient for eIF4E binding and translation inhibition. This is consistent with our observation that the whole proteins do not require a folded structure for binding or inhibition and with the model described above.

## DISCUSSION

We have shown that the 4E-BPs bind to eIF4E without folded structure and that the same protein samples are able to inhibit translation. This conflicts with the common assumption that proteins require folded structure for their biological activity. A few proteins are unstructured under physiological conditions but fold upon binding to their

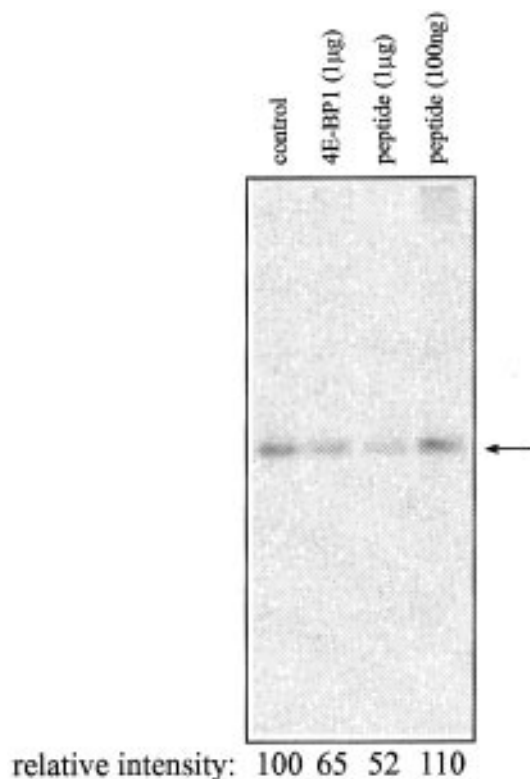


FIGURE 5: A 20 residue fragment of 4E-BP1 inhibits translation in vitro. SDS-PAGE gel of  $^{35}\text{S}$ -labeled protein produced by translation of capped CAT mRNA in reticulocyte lysate. In the control experiment no 4E-BP1 or peptide was included. In other cases the translation mixture contained the indicated amount of histidine tagged rat 4E-BP1 or the 4E-BP1 peptide. This experiment was repeated with similar results.

ligands (reviewed in ref 34). Also, an unfolded peptide fragment of the cell cycle regulator p21 adopts a rigid extended conformation upon binding to its target protein PCNA (35, 36). However, the 4E-BPs appear to be the first examples of whole proteins that bind and function without folded structure at any stage.

Although this seems surprising, it is similar to the flexible binding loops found in many folded proteins, except that there is no framework of folded structure to present the binding residues in a particular way. This rules out the possibility of complementary shape contributing to the binding affinity and specificity, making the interaction an extreme example of an induced fit. Another interesting implication of the lack of structure is that it rules out the possibility of allosteric control of 4E-BP activity. This implies that the phosphorylation sites responsible for dissociation from eIF4E are close in sequence to the binding site.

Can an unfolded protein be stable in vivo? This is an important consideration since in the absence of mitogenic stimuli the 4E-BPs must be present at high enough levels to prevent uncontrolled growth. The available knowledge of proteolytic degradation in eukaryotic cells suggests that an unfolded protein may be no more susceptible than a folded one, since these processes either recognize specific sequence motifs (e.g., the PEST motifs mentioned below) or involve indiscriminate harvesting of a region of the cytoplasm for breakdown in lysosomes (37). Regarding nonenzymatic chemical degradation, oxidation is no more likely than for

any exposed thiol group and the rates of aspartate and asparagine deamidation are fairly slow, although they are somewhat faster in unstructured peptides than in folded proteins (38). Thus, there seems to be no compelling reason why an unfolded protein cannot be stable in the cell.

Our results suggest that a small central region of the 4E-BPs binds to eIF4E while the rest is unfolded and flexible. However, it seems unlikely that the terminal regions of the proteins have no function, since the entire sequences have been highly conserved during mammalian evolution. What role might the terminal regions play in the absence of a requirement for a folded structure? They might carry out additional activities required for translation inhibition or even completely separate, as yet undiscovered, functions. One possibility is suggested by the sequence of the proteins. They contain PEST motifs flanking the eIF4E binding region: 4E-BP1 residues 21–50 and 74–96 and 4E-BP2 residues 33–50 and 64–91. These motifs are characterized by an abundance of proline, glutamate, aspartate, serine, and threonine residues in a region bound by a pair of basic amino acids. They are typically found in short-lived proteins and have been proposed to make them targets for degradation by the  $\text{Ca}^{2+}$  activated protease calpain (39, 40). It is therefore possible that PEST motifs in the flanking regions are important for regulating 4E-BP turnover.

## REFERENCES

1. Pause, A., Belsham, G. J., Gingras, A.-C., Donzé, O., Lin, T.-A., Lawrence, J. C., Jr., and Sonenberg, N. (1994) *Nature* 371, 762.
2. Merrick, W. C., and Hershey, J. W. B. (1996) in *Translational Control* (Hershey, J. W. B., Mathews, M. B., and Sonenberg, N., Eds.) pp 31–69, Cold Spring Harbor Laboratory Press, Plainview, New York.
3. Sonenberg, N. (1996) in *Translational Control* (Hershey, J. W. B., Mathews, M. B., and Sonenberg, N., Eds.) pp 245–269, Cold Spring Harbor Laboratory Press, Plainview, New York.
4. Brooks, R. F. (1977) *Cell* 12, 311.
5. Haghighat, A., Mader, S., Pause, A., and Sonenberg, N. (1995) *EMBO J.* 14, 5701.
6. Mader, S., Lee, H., Pause, A., and Sonenberg, N. (1995) *Mol. Cell. Biol.* 15, 4990.
7. Haystead, T. A., Haystead, C. M., Hu, C., Lin, T. A., and Lawrence, J. C., Jr. (1994) *J. Biol. Chem.* 269, 23185.
8. Fleurent, M., Gingras, A.-C., Sonenberg, N., and Meloche, S. (1997) *J. Biol. Chem.* 272, 4006.
9. Fadden, P., Haystead, T. A., and Lawrence, J. C., Jr. (1997) *J. Biol. Chem.* 272, 10240.
10. Lin, T. A., Kong, X., Haystead, T. A., Pause, A., Belsham, G., Sonenberg, N., and Lawrence, J. C., Jr. (1994) *Science* 266, 653.
11. Lin, T. A., Kong, X., Saltiel, A. R., Blackshear, P. J., and Lawrence, J. C., Jr. (1995) *J. Biol. Chem.* 270, 18531.
12. Graves, L. M., Bornfeldt, K. E., Argast, G. M., Krebs, E. G., Kong, X., Lin, T. A., and Lawrence, J. C., Jr. (1995) *Proc. Natl. Acad. Sci. U.S.A.* 92, 7222.
13. von Manteuffel, S. R., Gingras, A.-C., Ming, X.-F., Sonenberg, N., and Thomas, G. (1996) *Proc. Natl. Acad. Sci. U.S.A.* 93, 4076.
14. Beretta, L., Gingras, A.-C., Svitkin, Y. V., Hall, M. N., and Sonenberg, N. (1996) *EMBO J.* 15, 658.
15. Diggle, T. A., Moule, S. K., Avison, M. B., Flynn, A., Foulstone, E. J., Proud, C. G., and Denton, R. M. (1996) *Biochem. J.* 316, 447.
16. Brown, E. J., and Schreiber, S. L. (1996) *Cell* 86, 517.

17. Brunn, G. J., Hudson, C. C., Sekulic, A., Williams, J. M., Hosoi, H., Houghton, P. J., Lawrence, J. C., Jr., and Abraham, R. T. (1997) *Science* 277, 99.
18. Gingras, A.-C., Svitkin, Y., Belsham, G. J., Pause, A., and Sonenberg, N. (1996) *Proc. Natl. Acad. Sci. U.S.A.* 93, 5578.
19. Kerekatte, V., Smiley, K., Hu, B., Smith, A., Gelder, F., and de Benedetti, A. (1995) *Int. J. Cancer* 64, 27.
20. Miyagi, Y., Sugiyama, A., Asai, A., Okazaki, T., Kuchino, Y., and Kerr, S. J. (1995) *Cancer Lett.* 91, 247.
21. Rousseau, D., Gingras, A.-C., Pause, A., and Sonenberg, N. (1996) *Oncogene* 13, 2415.
22. Tsukiyama-Kohara, K., Vidal, S. M., Gingras, A.-C., Glover, T. W., Hanash, S. M., Heng, H., and Sonenberg, N. (1996) *Genomics* 38, 353.
23. Lin, T. A., and Lawrence, J. C., Jr. (1996) *J. Biol. Chem.* 271, 30199.
24. Hu, C., Pang, S., Kong, X., Velluca, M., and Lawrence, J. C., Jr. (1994) *Proc. Natl. Acad. Sci. U.S.A.* 91, 3730.
25. Whalen, S. G., Gingras, A.-C., Amankwa, L., Mader, S., Branton, P. E., Aebersold, R., and Sonenberg, N. (1996) *J. Biol. Chem.* 271, 11831.
26. Edery, I., Altmann, M., and Sonenberg, N. (1988) *Gene* 74, 517.
27. Matsuo, H., Li, H., McGuire, A. M., Fletcher, C. M., Gingras, A.-C., Sonenberg, N., and Wagner, G. (1997) *Nat. Struct. Biol.* 4, 717.
28. Sklenár, V., Piotto, M., Leppik, R., and Saudek, V. (1993) *J. Magn. Reson. A* 102, 241.
29. Mori, S., Abeygunawardana, C., Johnson, M. O., and van Zijl, P. C. M. (1995) *J. Magn. Reson. B* 108, 94.
30. Talluri, S., and Wagner, G. (1996) *J. Magn. Reson. A* 112, 200.
31. Wider, G., Macura, S., Kumar, A., Ernst, R. R., and Wüthrich, K. (1984) *J. Magn. Reson.* 56, 207.
32. Wishart, D. S., Sykes, B. D., and Richards, F. M. (1991) *J. Mol. Biol.* 222, 311–333.
33. Johnson, W. C., Jr. (1990) *Proteins* 7, 205.
34. Plaxco, K. W., and Gross, M. (1997) *Nature* 386, 657.
35. Chen, J., Peters, R., Saha, P., Lee, P., Theodoras, A., Pagano, M., Wagner, G., and Dutta, A. (1996) *Nucleic Acids Res.* 24, 1727.
36. Gulbis, J. M., Kelman, Z., Hurwitz, J., O'Donnell, M., and Kuriyan, J. (1996) *Cell* 87, 297.
37. Olson, T. S., Terlecky, S. R., and Dice, J. F. (1992) in *Stability of Protein Pharmaceuticals, Part B: In Vivo Pathways of Degradation and Strategies for Protein Stabilization* (Ahern, T. J., and Manning, M. C., Eds.) pp 89–118, Plenum Press, New York.
38. Clarke, S., Stephenson, R. C., and Lowenson, J. P. (1992) in *Stability of Protein Pharmaceuticals, Part B: In Vivo Pathways of Degradation and Strategies for Protein Stabilization* (Ahern, T. J., and Manning, M. C., Eds.) pp 1–29, Plenum Press, New York.
39. Rogers, S., Wells, R., and Rechsteiner, M. (1986) *Science* 234, 364.
40. Wang, K. K. W., Villalobo, A., and Roufogalis, B. D. (1989) *Biochem. J.* 262, 693.
41. Altmann, M., Schmitz, N., Berset, C., and Trachsel, H. (1997) *EMBO J.* 16, 1114.

BI972494R